iScience

CellPress
OPEN ACCESS

Article

Going against the family: Perturbation of a greenbeard pathway leads to falsebeard cheating

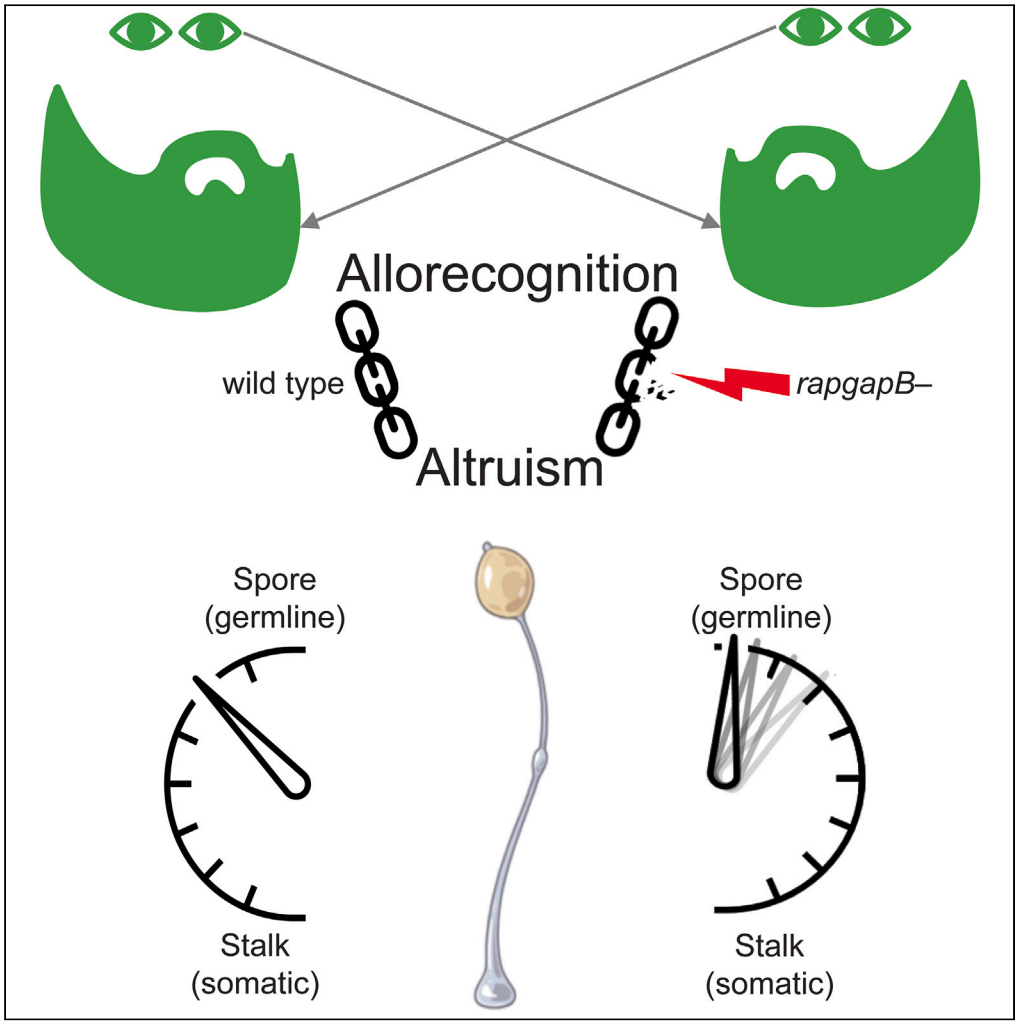

Peter Lehmann, Mariko Katoh-Kurasawa, Peter Kundert, Gad Shaulsky

gadi@bcm.edu

Highlights

Mutual suppression indicates that *rapgapB* is a component of the *tgrB1-tgrC1* pathway

rapgapB inactivation confers cheating by stalk avoidance and increased sporulation

rapgapB cheating does not alter the victim's cell-type proportioning

rapgapB cheating is allotype specific

rapgapB is an empirical demonstration of the falsebeard hypothesis

Lehmann et al., iScience *27*, 111125
November 15, 2024 © 2024 The Author(s). Published by Elsevier Inc.
https://doi.org/10.1016/j.isci.2024.111125

iScience

CellPress
OPEN ACCESS

Article

Going against the family: Perturbation of a greenbeard pathway leads to falsebeard cheating

Peter Lehmann,[1,2] Mariko Katoh-Kurasawa,[1] Peter Kundert,[1,2] and Gad Shaulsky[1,3,*]

SUMMARY

Greenbeards facilitate cooperation by encoding a perceptible signal, the ability to detect it, and a tendency to help others that display it. Falsebeards are hypothetical cheaters that display the signal without being altruistic. Despite many examples of greenbeards, evidence for falsebeards is scarce. The *Dictyostelium discoideum tgrB1-tgrC1* allorecognition pathway encodes a greenbeard. It allows development, which yields fruiting bodies with altruistic stalks that increase spore dispersal. Here we show that cells lacking *rapgapB*, a *tgrB1-tgrC1* signaling element, cheat by avoiding the stalk fate and generating more spores in chimeras than in pure populations. *rapgapB*$^-$ cells cheat only on partners with compatible *tgrB1-tgrC1* allotypes, suggesting that beard display and recognition are intact but decoupled from altruism. The *rapgapB*$^-$ falsebeard provides a model to study greenbeard maintenance and subversion.

INTRODUCTION

The greenbeard hypothesis was framed in the context of the seeming paradox inherent to altruistic cooperation, specifically that such cooperation might incentivize the emergence of mutations that allow individuals to reap the benefits of a common good without paying the full altruistic price to produce the good. By linking the beard signal to the capacity to cooperate altruistically (or to harm others that do not display the signal), a greenbeard ensures that altruism is only accessible to individuals capable of reciprocating altruistically.[1–3] The *tgrB1-tgrC1* allorecognition system of *Dictyostelium discoideum* is a complete example of a greenbeard.[4,5] During multicellular development, cells express the highly polymorphic transmembrane proteins TgrB1 and TgrC1. TgrB1 acts as a receptor that binds specifically to the TgrC1 ligand on the surface of neighboring cells, but only if TgrB1 and TgrC1 are of a matching allotype.[6–8] Allotype-compatible cells continue to cooperate during development, forming structures in which roughly 80% of the cells differentiate into germline spores and the remaining 20% generate a stalk that holds the spores aloft and facilitates dispersal. The mature somatic stalk is composed of dead vacuolized cells, so differentiation into stalk is an altruistic act that generates a common good.[9]

Falsebeards have been considered as hypothetical aberrations of greenbeard systems. A falsebeard is a genotype in which the greenbeard signal remains intact and functional but has been decoupled from the capacity to cooperate normally in production of the common good.[10–12] It was therefore interesting to identify downstream elements of the *tgrB1-tgrC1* signaling pathway that could link the display and perception of the greenbeard signal to the ability to participate in generating the stalk. Additionally, if any of these downstream elements altered cooperative behavior when genetically altered, it would be evidence for the existence of a falsebeard.

Genetic suppression is often used to identify additional nodes in a genetic pathway of interest.[13–15] When mutation of a known member of the pathway results in a mutant phenotype clearly distinguishable from the wild type, any additional genetic perturbation that restores the wild-type phenotype and suppresses the mutant phenotype would potentially be a mutation in another member of the pathway. By introducing mutations randomly throughout the genome, screening for mutants with wild-type phenotype, and mapping the genomic location of these mutations, it is possible to identify multiple candidate genes that could be important components of the pathway.

Previous work used various suppressor screen strategies to identify genetic modifiers of the *tgrB1-tgrC1* pathway.[16–18] A strain with a mismatched pair of *tgrB1-tgrC1* alleles arrests at the loose aggregate stage of development, just like the respective null alleles. Such a mismatch strain was subjected to chemical mutagenesis and the mutant pool was screened for emergence of developmental morphology resembling the wild type. The strongest signal recovered was a spectrum of mutations within the gene *rapgapB*.[17,19] RapGAPB is an effector of RapA activity in *D. discoideum*, potentially affecting cell motility and cytoskeletal remodeling dynamics. *rapgapB* inactivation affects the differentiation and spatial patterning of prestalk cells,[20] but its role in social behavior and its potential place in the *tgrB1-tgrC1* pathway have not been examined. Some of the mutations in the suppressor screen produced recessive loss-of-function alleles that were readily complemented with a wild-type allele of *rapgapB*, and some produced dominant negative alleles.[17] We therefore hypothesized that *rapgapB* is a proximal,

[1]Department of Molecular and Human Genetics, Baylor College of Medicine, Houston, TX 77030, USA
[2]Graduate program in Genetics and Genomics, Baylor College of Medicine, Houston, TX 77030, USA
[3]Lead contact
*Correspondence: gadi@bcm.edu
https://doi.org/10.1016/j.isci.2024.111125

This is an open access article under the CC BY-NC license (http://creativecommons.org/licenses/by-nc/4.0/).

downstream element of the *tgrB1-tgrC1* greenbeard pathway, and that *rapgapB* inactivation might uncouple the greenbeard signaling and signal reception from the altruistic aspects of the pathway.

Cheating is broadly defined as benefiting from social cooperation without fully paying the associated cost.[21–23] In *D. discoideum*, most cheaters have been defined more stringently as individuals that produce more spores than their victims in an equal mix.[24–26] Nevertheless, the broader definition can be useful even if the cheater does not produce more spores than its victim. For example, inactivation of *tgrB1* causes cheating in that the *tgrB1*$^-$ strain, which produces very few spores on its own, benefits from the social cooperation by producing many spores when mixed with the wild type.[5] Moreover, the *tgrB1*$^-$ strain does not pay the full cost of cooperation because it does not contribute significantly to the stalk. The wild type, which makes most of the stalk cells, does pay the associated cost, but it still produces more spores than the *tgrB1*$^-$ strain in the mix. Therefore, *tgrB1*$^-$ cells are cheaters because they benefit from the social cooperation without paying the full cost, but they could be considered partial cheaters because they do not make more spores than the wild type.[5] Another aspect that is not often considered in the definition of *D. discoideum* cheaters is the long-term consequence of cheating. In the case of *tgrB1*$^-$, it has been proposed that the wild-type victim suffers an additional cost after the spores germinate because the germinating *tgrB1*$^-$ spores compete with the wild type for environmental resources such as space and food.[5]

Here, we show that *rapgapB* is a member of the *tgrB1-tgrC1* pathway because *rapgapB* inactivation suppresses the developmental defects caused by inactivation of the *tgrB1-tgrC1* pathway. We show that inactivation of *rapgapB* causes partial cheating because the *rapgapB*$^-$ mutant makes more spores when mixed with the wild type than it does when developed on its own. Moreover, the *rapgapB*$^-$ mutant does not contribute significantly to the stalk when co-developed with the wild type. We also show that the *rapgapB*$^-$ mutant only cheats on cells that share its *tgrB1-tgrC1* allotype. These findings support the conclusion that *rapgapB* inactivation causes a falsebeard phenotype, thus further supporting the greenbeard hypothesis.

RESULTS

rapgapB is a component of the *tgrB1-tgrC1* signaling pathway

To explore the possible role of *rapgapB* in social behavior, we knocked it out in an otherwise wild-type AX4 background via CRISPR-Cas9 and compared the developmental morphology and progression of the resulting strain to AX4, *tgrB1*$^-$, and *tgrC1*$^-$ when developed on black filters (Figures 1A–1D). The developmental progression of the *rapgapB*$^-$ strain was delayed, exhibiting loose aggregates at 16 h when the wild type already forms fingers (Figures 1A and 1B, 16 h). It then progressed to a multi-tipped aggregate stage and largely arrested there, with a minority of small fruiting bodies with short gnarled stalks, while the wild type formed well-proportioned fruiting bodies (Figures 1A and 1B, 24 h). The morphology of *rapgapB*$^-$ resembled *tgrB1*$^-$ and *tgrC1*$^-$ through the first 16 h post-starvation. The phenotype diverged from *tgrB1*$^-$ and *tgrC1*$^-$, which remained arrested at the loose aggregate stage after 24 h. The *rapgapB*$^-$ strain formed distinctive clustered aggregates at 20 h and beyond (Figure S1B), a morphology that is not typically seen in the wild type or in the other mutants.

Mutations in *rapgapB* can suppress the developmental arrest observed in a strain that contains a pair of non-matching alleles of *tgrB1* and *tgrC1*.[17] To determine whether *rapgapB*$^-$ can also suppress the developmental arrest phenotypes of *tgrB1*$^-$ and *tgrC1*$^-$, we knocked out *rapgapB* in the respective strains. The resulting double-knockout strains formed fingers at 16 h and fruiting bodies at 24 h (Figures 1E and 1F), exhibiting developmental morphology and progression that were more similar to AX4 than to *rapgapB*$^-$, *tgrB1*$^-$, or *tgrC1*$^-$. The double-knockout strains were also morphologically similar to AX4 throughout the developmental time course, but notably generated a more variable and asynchronous population of structures (Figures S1E and S1F).

To quantify the developmental outcomes, we developed the cells on black filters for 40 h, counted the spores, and calculated the sporulation efficiencies. We found that *rapgapB*$^-$ was severely deficient in spore production compared to AX4, much like *tgrB1*$^-$ and *tgrC1*$^-$. For *rapgapB*$^-$ *tgrB1*$^-$ and *rapgapB*$^-$ *tgrC1*$^-$, we quantified the sporulation efficiencies of two independently isolated clones. These double-knockout strains produced more spores than either of the respective single-knockout strains, though not quite equivalent to AX4 (Figure 1G). The statistical significance of the differences between the strains is shown in Table S4.

The results in Figure 1 show that *rapgapB*$^-$ is a mutual suppressor of both *tgrB1*$^-$ and *tgrC1*$^-$, suggesting that *rapgapB* is a member of the *tgrB1-tgrC1* developmental pathway.

Inactivation of *rapgapB* confers partial cheating

The *tgrB1-tgrC1* pathway is a key regulator of *D. discoideum* social cooperation. Finding that *rapgapB* is a component of that pathway in development prompted us to hypothesize that *rapgapB* inactivation might also affect social cooperation. We therefore tested the social behavior of *rapgapB*$^-$ in a chimeric mix with AX4. We mutated *rapgapB* in an otherwise wild-type strain constitutively labeled with mCherry, and mixed it in equal proportions with AX4-GFP. We developed the mixed strains and followed the position of the labeled cells. In the chimeric slugs (Figure 2A), *rapgapB*$^-$ mCherry was almost completely absent from the anterior (A) prestalk region, and abundant in the posterior (P) prespore region. The AX4-GFP cells were enriched in the anterior region and in the rear guard region, which are normally enriched in prestalk cells. In the terminal fruiting body (Figure 2B), *rapgapB*$^-$ mCherry was largely absent from the stalk (St) and the upper cup (UC), which are prestalk-derived structures. It was enriched in the spore mass (Sp), whereas the AX4-GFP cells were enriched in the stalk and in the upper cup. In contrast, a control mix between AX4-GFP and AX4-mCherry resulted in equal and uniform distribution of both mixing partners throughout all compartments of the slug and fruiting body (Figures 2C and 2D). We also performed a fluorescent marker swap experiment to rule out the possibility that localization of *rapgapB*$^-$ could be attributable to the fluorescent marker. We mutated *rapgapB* in AX4-GFP using the same vector as was used on AX4-mCherry. We then mixed the resulting *rapgapB*$^-$ GFP strain at equal proportions with

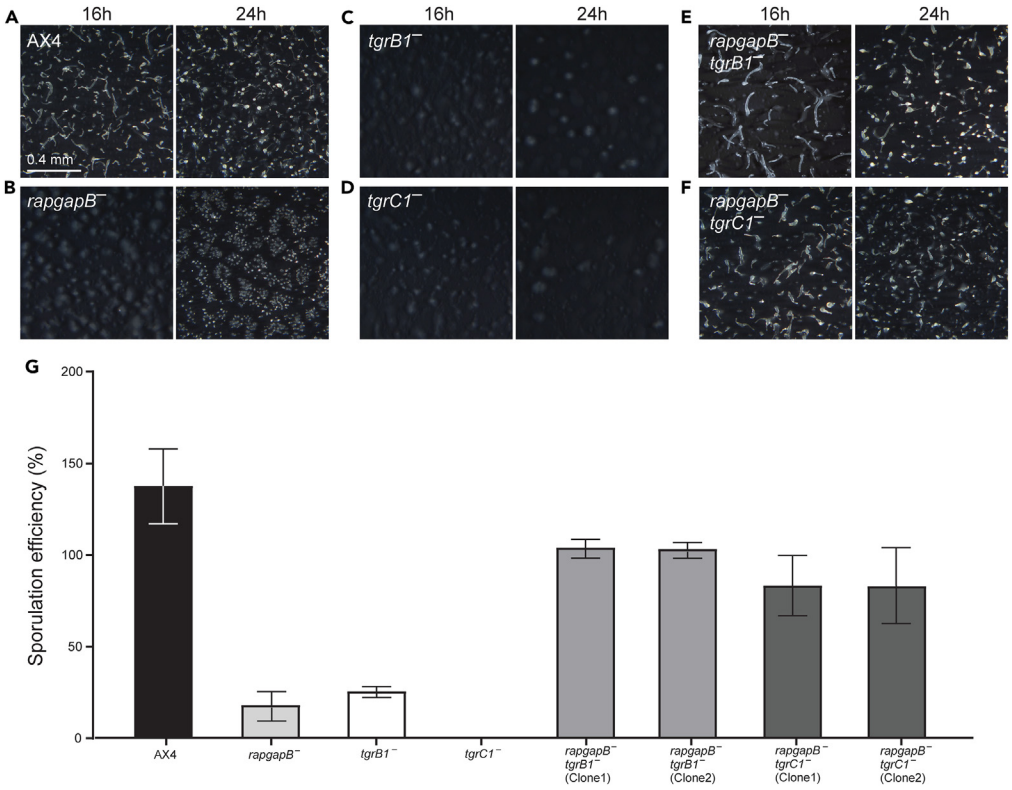

Figure 1. *rapgapB* is a component of the *tgrB1-tgrC1* pathway

We used CRISPR-Cas9 to knock out *rapgapB* in the wild type (AX4) as well as in the *tgrB1*– and *tgrC1*– strains, developed the mutant strains on black nitrocellulose filters and photographed them through a dissecting microscope from above. We compared developmental morphology at 16 h and 24 h post-starvation of AX4 (A) to *rapgapB*– (B), *tgrB1*– (C), *tgrC1*– (D), *rapgapB*– *tgrB1*– Clone 1 (E), and *rapgapB*– *tgrC1*– Clone 1 (F). We also separately developed 5 × 10^6 cells of each of these strains on black nitrocellulose filters, counted the spores present on each filter at 40 h post-starvation and calculated them as a percentage of the initial number of cells placed on the filter (sporulation efficiency) (G). The average sporulation efficiency (y axis) is represented by bar heights, the whiskers represent the standard deviation of the independent replicates (AX4 and *rapgapB*–: $n = 6$ each; all others: $n = 3$ each), and the strain names are indicated below the respective bars (x axis). Statistical significance data are shown in Table S4. Source data are provided in Table S6.

AX4-mCherry and observed the localization of each mixing partner within slugs and fruiting bodies (Figure S2). This reciprocal fluorescent strain mixture also showed strong localization of *rapgapB*⁻ to the prespore and spore regions, confirming that this behavior is independent of the fluorescent marker used. We therefore conclude that *rapgapB*⁻ preferentially adopts the prespore fate when mixed with AX4, and that this behavior is not affected by the fluorescent marker.

To quantify the developmental outcomes, we developed the cells on black filters for 40 h, counted the spores, and calculated their sporulation efficiencies. We found that *rapgapB*⁻ mCherry produced roughly 14-fold more spores when codeveloped with the wild-type partner than it did in a pure population. It also produced 12% more spores than AX4 in the mix (Figure 2E), although the difference was not statistically significant (t test, $p = 0.144$) and there was no significant reduction in AX4 sporulation. We also tested the social behavior of a *rapgapB*⁻ strain that was generated by insertional mutagenesis.[20] Figure S3 shows that the *rapgapB*⁻ mutant increased its sporulation efficiency 2.9-fold in the mix and the sporulation efficiency of AX4 was reduced 2.3-fold. Moreover, the mutant produced 35% more spores than AX4. Together these experiments suggest that *rapgapB*⁻ is a partial cheater because loss of *rapgapB* results in avoiding the prestalk fate and forming more than its fair share of spores when mixed with a wild-type partner.

Effects of *rapgapB*⁻ cheating on prespore/prestalk differentiation

The partial cheating behavior of *rapgapB*⁻ in mixes prompted us to track the prespore and prestalk cells in the cheater and its victim within chimeras. We generated two separate expression vectors, one driving mCherry expression via the promoter of the canonical prespore-specific gene *cotB*, and the other driving mNeonGreen expression via the promoter of the canonical prestalk-specific gene *ecmA*. We co-transformed these vectors into AX4 to allow visualization of prespore and prestalk compartments, and tracking of individual cell fate history.

In AX4, *[ecmA]*:mNeonGreen labeled the anterior prestalk region of the slug and sporadic cells within the posterior region, consistent with anterior-like cells, while *[cotB]*:mCherry labeled the posterior prespore compartment (Figure 3A). In the terminal fruiting body, *[ecmA]*:mNeonGreen labeled the entire stalk as well as the upper and lower cups, while *[cotB]*:mCherry labeled the vast majority of the spores

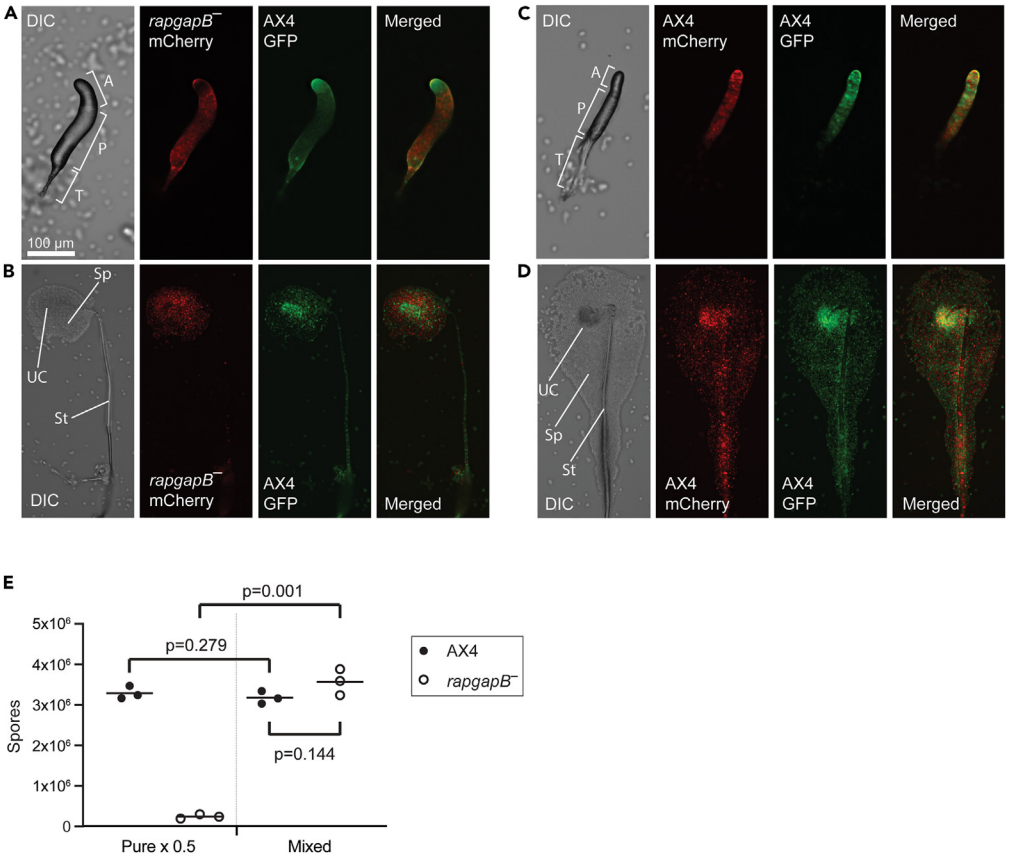

Figure 2. Inactivation of *rapgapB* confers cheating behavior

We used two strains that express constitutive fluorescent markers, the wild-type AX4-GFP (green) and the mutant *rapgapB*⁻ mCherry (red). We grew the cells separately, mixed equal proportions, and co-developed them. We imaged the structures at the finger (A) and fruiting body stage (B) with differential interference contrast (DIC) microscopy and with green and red fluorescence, and generated a merged image of the red and green channels as indicated. As a control, we co-developed constitutively labeled wild-type AX4 GFP cells (green) with constitutively labeled wild-type AX4 mCherry cells (red). We imaged the structures at the finger (C) and fruiting body stage (D) as described previously. We imaged fruiting bodies that have fallen over to better illustrate their anatomy. In (A) and (C), we show the anterior (A) of the slug that contains mainly prestalk cells, the posterior (P) that contains mainly prespore cells, and the trail (T) that contains few or no cells. In (B) and (D), we show the upper cup (UC) that contains mainly prestalk cells, the spores (Sp) and the stalk (St).

(E) We grew wild-type AX4-GFP and mutant *rapgapB*⁻ mCherry cells separately, developed 5×10^6 cells either in pure populations or mixed at equal proportions as indicated (x axis), and counted spores. The spore counts (y axis) are shown as three independent replicates (symbols) and their averages (horizontal lines). The pure population counts were multiplied by 0.5 to scale them with the mixed population. Brackets and *p* values (t test, $n = 3$) compare the spore counts of each strain in the two conditions (above) and the spore counts of the two strains in the mix (below). Camera settings are included in Table S1. Source data are provided in Table S6.

(Figure 3B). We imaged fruiting bodies that have been collapsed onto the substrate to show the structures more easily in a single focal plane. Occasional *[cotB]*:mCherry foci were found alongside the *[ecmA]*:mNeonGreen-labeled stalk due to stray *[cotB]*:mCherry-positive spores that came to rest next to the stalk after the fruiting body collapsed. We did not observe any stalk cells expressing the prespore marker *[cotB]*:mCherry, nor did we observe the prestalk signal of *[ecmA]*:mNeonGreen in any spores. We also disaggregated populations of mature fruiting bodies and counted the spores with fluorescence microscopy (Table S5). More than 97% of the spores were labeled with *[cotB]*:mCherry and none were labeled with *[ecmA]*:mNeonGreen.

When we introduced the *rapgapB*⁻ mutation into the dual-labeled AX4 strain, it formed primarily multi-tipped aggregates (Figure 3C), consistent with the morphology of the unlabeled *rapgapB*⁻ (Figure S1B). The cells weakly and sporadically expressed the prestalk and prespore reporters without much separation between the cell types (Figure 3C). While a large majority of the cells remained at that stage, rare small fruiting bodies were formed occasionally (Figure 3D). Most of the spores in these fruiting bodies did not express *[cotB]*:mCherry and most of the stalk cells were not labeled with *[ecmA]*:mNeonGreen. When *[ecmA]*:mNeonGreen labeling was present, it was consistently stronger near the base of the stalk. We also disaggregated the rare fruiting bodies and counted the spores with fluorescence microscopy (Table S5). About 17% of the spores were labeled with *[cotB]*:mCherry and none were labeled with *[ecmA]*:mNeonGreen. The findings in Figures 3C and 3D and in Table S5 suggest that *rapgapB*⁻ is deficient in expressing key prespore and prestalk differentiation markers even though it is capable of some terminal differentiation into spores and stalks.

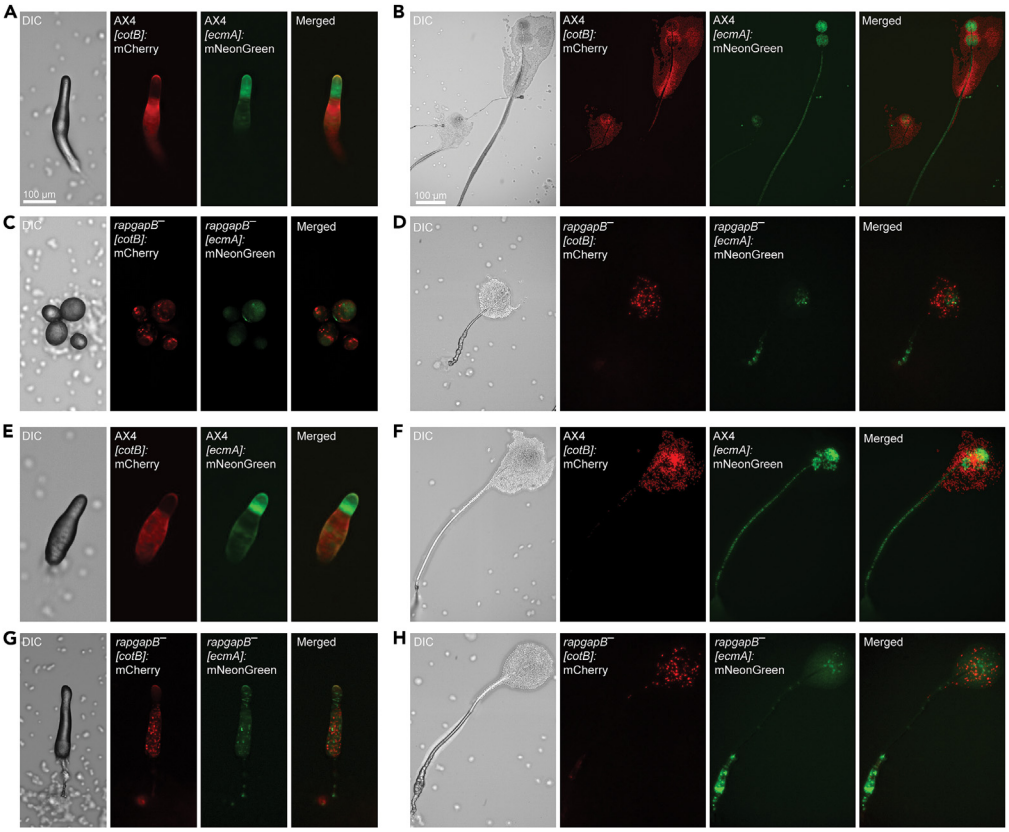

Figure 3. Cell-type development of the *rapgapB*⁻ cheater and its victim

We generated strains carrying the prestalk reporter *[ecmA]*:mNeonGreen (green) and the prespore reporter *[cotB]*:mCherry (red) in either the wild-type AX4 background or the *rapgapB*⁻ background. We imaged the structures of AX4 *[cotB]*:mCherry *[ecmA]*:mNeonGreen at the finger stage (A) and fruiting body stage (B), and the structures of *rapgapB*⁻ *[cotB]*:mCherry *[ecmA]*:mNeonGreen at the multi-tipped aggregate stage (C) and the rarely observed fruiting body stage (D), with DIC microscopy and with green and red fluorescence, and generated a merged image of the red and green channels as indicated. We codeveloped AX4 *[cotB]*:mCherry *[ecmA]*:mNeonGreen with unlabeled *rapgapB*⁻ cells after growing the two strains separately and mixing them in equal proportions. We imaged the structures at the finger stage (E) and fruiting body stage (F). We also codeveloped *rapgapB*⁻ *[cotB]*:mCherry *[ecmA]*:mNeonGreen with unlabeled AX4 cells and imaged the structures at the finger stage (G) and fruiting body stage (H). We imaged fruiting bodies that have fallen over to better illustrate their anatomy. The red staining at the tip of the slug anterior regions is due to reflection and is not associated with cells. Camera settings are included in Table S1. Source data are provided in Table S6.

We then codeveloped dual-labeled AX4 with unlabeled *rapgapB*⁻ to observe the effect of cheating on the victim's cell-type differentiation. Cell-type localization and abundance in the slug (Figure 3E) were indistinguishable from the pure population dual-labeled AX4, indicating no overt displacement or ectopic expression of cell-type markers in the mix. In the fruiting body (Figure 3F), roughly half the spores were *[cotB]*:mCherry-positive. We found no evidence for *[cotB]*:mCherry expression in the stalk or *[ecmA]*:mNeonGreen expression in the spores, indicating the victim did not transdifferentiate from one cell type to the other. As with the pure population dual-labeled AX4, *[cotB]*:mCherry staining in the vicinity of the stalk indicated spores that dislodge from the sorus and came to rest near the stalk. Counting the spores showed that about 40% were labeled with *[cotB]*:mCherry (Table S5) and none were labeled with *[ecmA]*:mNeonGreen.

To evaluate the cell-type differentiation of the partial cheater in the chimeras, we codeveloped dual-labeled *rapgapB*⁻ with unlabeled AX4. Expression of both fluorophores was punctate and sparse within the slug, such that individual high-expressing cells were easily discernible among their non-expressing neighbors (Figure 3G). Sporadic expression of the cell-type markers continued to the fruiting body stage (Figure 3H), where the stalk and prestalk-derived structures were mostly *[ecmA]*:mNeonGreen-negative and the spores were largely *[cotB]*:mCherry-negative. Further examination revealed about 7% *[cotB]*:mCherry-positive spores and no *[ecmA]*:mNeonGreen-positive spores (Table S5). We conclude that while the presence of a wild-type victim greatly improves *rapgapB*⁻ sporulation, the improvement is not accompanied by a restoration of cell-type marker expression to wild-type levels. We also did not observe any evidence for transdifferentiation (conversion of prespore to prestalk or vice versa) in the cheater or in the victim.

We observed a significant *mNeonGreen* signal at the base of fruiting bodies formed by *rapgapB*⁻ *[cotB]*:mCherry *[ecmA]*:mNeonGreen, both in pure population (Figure 3D) and when mixed 50:50 with unlabeled AX4 (Figure 3H). Surprisingly, we did not observe overrepresentation of *rapgapB*⁻ cells in the base of the fruiting body when we labeled the *rapgapB*⁻ cells with the constitutive fluorescent markers

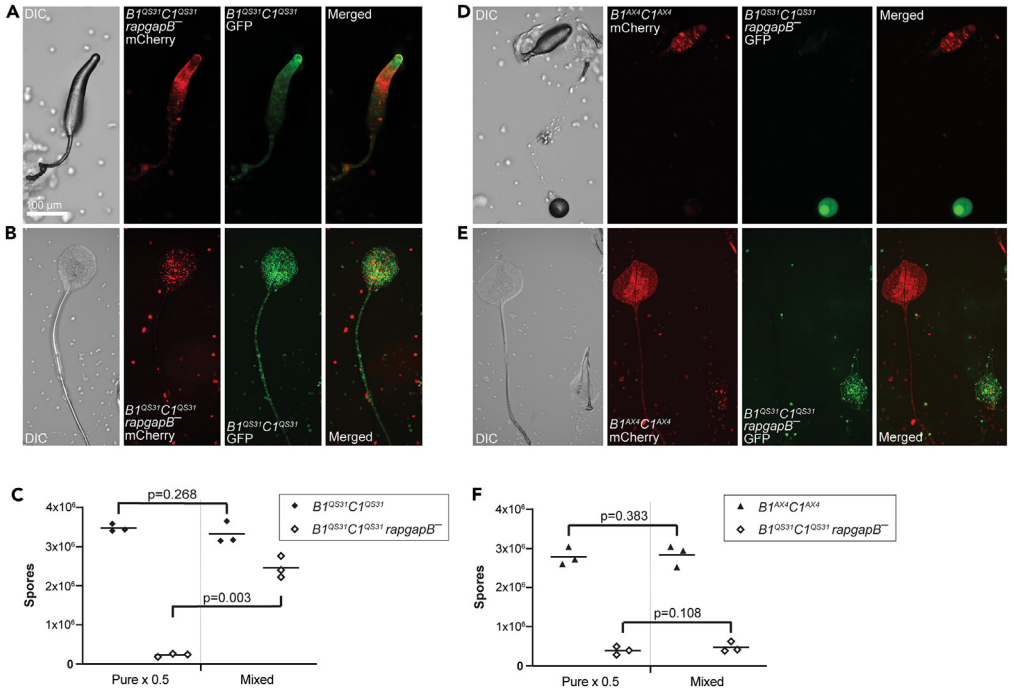

Figure 4. *rapgapB*⁻ cheating is allotype-specific

We used strains that express constitutive GFP (green) or mCherry (red) markers, in which we replaced the resident *tgrB1-tgrC1* locus with a control locus from AX4 ($B1^{AX4}C1^{AX4}$) or a different allotype locus from QS31 ($B1^{QS31}C1^{QS31}$). We then knocked out *rapgapB* in the marked $B1^{QS31}C1^{QS31}$ strains. In each experiment we grew the cells separately, mixed equal proportions, and co-developed them. We imaged the structures at the finger (A and D) and fruiting body stage (B and E) with DIC microscopy and with green and red fluorescence, and generated a merged image of the red and green channels as indicated. In (A) and (B), the $B1^{QS31}C1^{QS31}$ *rapgapB*⁻ mutant is labeled in red and mixed with a compatible $B1^{QS31}C1^{QS31}$ strain which is labeled in green. In (D) and (E), the $B1^{QS31}C1^{QS31}$ *rapgapB*⁻ mutant is labeled in green and mixed with an incompatible $B1^{AX4}C1^{AX4}$ strain that is labeled in red. We also used the respective strains to test sporulation efficiency.

(C) Compatible $B1^{QS31}C1^{QS31}$ *rapgapB*⁻ and $B1^{QS31}C1^{QS31}$.

(F) Incompatible $B1^{QS31}C1^{QS31}$ *rapgapB*⁻ and $B1^{AX4}C1^{AX4}$. In each case, we developed 5×10^6 cells either in pure populations or mixed at equal proportions as indicated, and counted spores. The spore counts are shown as three independent replicates (symbols) and their averages (horizontal lines). The pure population counts were multiplied by 0.5 to scale them with the mixed population. Brackets and *p* values (t test, $n = 3$) compare the spore counts of each strain in the two conditions. The *p* value for the comparison between $B1^{QS31}C1^{QS31}$ and $B1^{QS31}C1^{QS31}$ *rapgapB*⁻ in the mix (C) is 0.036 and the *p* value for the comparison between $B1^{AX4}C1^{AX4}$ and $B1^{QS31}C1^{QS31}$ *rapgapB*⁻ (F) is 0.002 (not shown in the graph). Camera settings are included in Table S1. Source data are provided in Table S6.

[act15]:mCherry (Figure 2) and *[act15]*:GFP (Figure S2). The reasons for this observation are unclear, but this potential discrepancy appears to occur in a small sub-population of cells. It does not appear to affect our broader observation that *rapgapB*⁻ cells largely avoid contributing to the common good of the stalk and partially cheat on the wild type.

Allotype compatibility is required for partial cheating by *rapgapB*⁻

To assess whether the partial cheating behavior of *rapgapB*⁻ is dependent on the *tgrB1-tgrC1* allotypes of the interacting strains, we introduced the *rapgapB*⁻ mutation into a strain in which the resident *tgrB1-tgrC1* locus of AX4-mCherry was replaced by the *tgrB1-tgrC1* locus of QS31, a wild isolate of *D. discoideum*.[7] This QS31 allotype was chosen because it is highly distinct from AX4, both in its degree of sequence dissimilarity at the *tgrB1-tgrC1* locus and because it strongly segregates from AX4 cells when codeveloped in a chimeric mix. The resulting strain ($B1^{QS31}C1^{QS31}$ *rapgapB*⁻ mCherry) was mixed in equal proportion with $B1^{QS31}C1^{QS31}$ GFP and the cells were developed together. $B1^{QS31}C1^{QS31}$ *rapgapB*⁻ mCherry was notably absent from the anterior prestalk region of the slug (Figure 4A) as well as the prestalk-derived cup structures and the stalk of the terminal fruiting body (Figure 4B). Spore quantification revealed that $B1^{QS31}C1^{QS31}$ *rapgapB*⁻ mCherry produced almost 11-fold more spores within a chimera with an allotype-compatible partner than it did in a pure population (Figure 4C). The pre-spore-biased sorting behavior and increased spore production of $B1^{QS31}C1^{QS31}$ *rapgapB*⁻ mCherry mirrors the results of the *rapgapB*⁻ mutation within the AX4 allotype (Figure 2). It also shows that the partial cheating behavior conferred by *rapgapB*⁻ is not specific to the AX4 allotype and likely does not vary greatly across different allotypes.

To test whether *rapgapB*⁻ confers cheating behavior by bypassing allorecognition or leaves allorecognition intact, we assayed the behavior of *rapgapB*⁻ when mixed with an incompatible strain. We generated the strain $B1^{QS31}C1^{QS31}$ *rapgapB*⁻ GFP and mixed it with a strain that underwent a control double gene replacement process to carry the *tgrB1-tgrC1* locus of AX4 ($B1^{AX4}C1^{AX4}$ mCherry). The two strains

formed almost completely separate structures of $B1^{AX4}C1^{AX4}$ mCherry slugs and $B1^{QS31}C1^{QS31}$ *rapgapB*$^{-}$ GFP tipped aggregates (Figure 4D). At the fruiting body stage, the two strains remained in mostly separate structures (Figure 4E). Quantification of spores from these fruiting bodies revealed no significant change in sporulation of either mixing partner between pure population and chimera (Figure 4F). Instead, each allotype-incompatible partner developed and sporulated regardless of the presence of the other.

The results shown in Figure 4 suggest that partial cheating by *rapgapB*$^{-}$ depends on allotypic compatibility between the interacting strains.

DISCUSSION

We have shown previously that the *tgrB1-tgrC1* locus exhibits the key characteristics of a greenbeard system, namely the ability to display an unusual signal, the ability to perceive that signal, and the tendency to act altruistically toward others that display the same signal.[5] We have now found that *rapgapB* inactivation confers behavior consistent with a direct subversion of that greenbeard system. The conversion of a perceived honest signal into a dishonest one makes *rapgapB*$^{-}$ an example of a falsebeard.[10–12]

Fulfillment of the falsebeard role was observed in *rapgapB*$^{-}$ in three ways. First, *rapgapB* was epistatically linked to the *tgrB1-tgrC1* pathway because its inactivation suppressed the developmental consequences of *tgrB1* and *tgrC1* loss of function. Second, *rapgapB*$^{-}$ gained partial advantage over allotype-compatible partners by avoiding contributing to the common good of the prestalk niche. It also produced manyfold more spores in chimeras with a wild-type victim than it could produce on its own. Third, the partial cheating behavior of *rapgapB*$^{-}$ was not observed toward an allotype-incompatible partner, indicating that this behavior requires an intact and faithful allorecognition signal. Therefore, the *rapgapB*$^{-}$ partial cheater acts by directly subverting the honesty of the *tgrB1-tgrC1* signal.

Most key characteristics that make *rapgapB*$^{-}$ a falsebeard are also present in the cheater *tgrB1*$^{-}$. The *tgrB1* gene is part of the greenbeard pathway, the *tgrB1*$^{-}$ mutant cheats on the wild-type partner, and the cheating is allotype-specific.[5] Nevertheless, *tgrB1* is the greenbeard receptor, which is essential for perceiving the beard "color." Therefore, allorecognition is not reciprocal in a mix between *tgrB1*$^{-}$ and the wild type—the wild-type partner recognizes the *tgrC1* signal displayed by the *tgrB1*$^{-}$ cells, but the *tgrB1*$^{-}$ mutant cannot recognize the wild-type cells. Whether *tgrB1*$^{-}$ should be considered a false signal-bearer is therefore confounded by the fact it is missing the receptor for such a signal. In contrast, the *rapgapB* gene is at least one step removed from the central *tgrB1-tgrC1* hub, so *rapgapB*$^{-}$ is unambiguously a falsebeard that acts in the context of an intact greenbeard signal-receptor system.

Our experiments revealed that *tgrB1*$^{-}$ and *tgrC1*$^{-}$ are mutual suppressors of *rapgapB*$^{-}$ because each mutation alone causes developmental defects that are suppressed in the respective double mutants. The mutual suppression observed in *rapgapB*$^{-}$ *tgrB1*$^{-}$ and *rapgapB*$^{-}$ *tgrC1*$^{-}$ was somewhat unexpected, because the genetic screen that revealed the suppression predicted a direct and linear epistatic relationship between *tgrB1-tgrC1* and *rapgapB*.[17] Mutual suppression has been observed in other organisms, where it usually suggests that the respective genes encode distinct subunits of a single protein complex or otherwise tightly linked in a genetic pathway.[14,15] While we have no evidence for physical interactions between TgrB1-TgrC1 and RapGAPB at the protein level, the genetic implication of the mutual suppression is that *rapgapB* is a proximal node in the *tgrB1-tgrC1* pathway.

Previous work on the role of *rapgapB* in development is concordant with our observation that *rapgapB*$^{-}$ was largely absent from prestalk regions and prestalk-derived structures when mixed with AX4.[20] Those studies focused on the effects of *rapgapB* loss-of-function on prestalk differentiation, patterning, cell motility, and adhesion, primarily in the context of the pure strain. Our results confirm the previous findings, and extend them by emphasizing the social behavior of *rapgapB*$^{-}$ in relation to other genotypes. While aberrant prestalk-specific patterning and differentiation can be understood as a defect in a pure population, in chimeric mixes the defect is recontextualized as a partial competitive advantage. Because of its incompetence at forming stalk, *rapgapB*$^{-}$ does not pay the fair cost of cooperation but still benefits from increased spore production.

The role of *rapgapB* in development and the molecular mechanisms that tie it to the *tgrB1-tgrC1* pathway are somewhat unclear. The three genes are expressed only during development and their peak expression times are between 8 and 12 h of development,[6,27] around the time cells transition from loose aggregates to tight aggregates. RapgapB is a developmental regulator of RapA, which is a master regulator of many cellular functions during growth and development.[20,28] TgrB1 and TgrC1 function as a ligand-receptor pair,[8] but there is no known relationship between *tgrB1-tgrC1* and *rapgapB-rapA* other than the data described here. Nevertheless, there are interesting similarities between the phenotypes of the mutant strains that suggest involvement of extracellular signals. Most prominently, *tgrB1*$^{-}$ and *rapgapB*$^{-}$ cells exhibit developmental defects that manifest around the loose-aggregate to tight-aggregate transition. Moreover, as shown here and in previous work, both strains gain the ability to produce spores in the presence of wild-type cells.[5] The non-cell autonomous nature of these mutations suggests the involvement of an extracellular signal of an unknown identity.

The molecular mechanism by which *rapgapB*$^{-}$ cheats on AX4 remains unclear. Transdifferentiation of either strain is unlikely, because we did not find spores of *rapgapB*$^{-}$ or stalk cells of AX4 that were *ecmA* and *cotB* double-positive within chimeric mixes. The weak and sporadic expression of *cotB* in *rapgapB*$^{-}$ appears to be unchanged in chimera versus pure population, suggesting that co-development with AX4 does not restore normal expression of the prespore differentiation program despite the dramatic increase in the number of mature spores. It is possible that the incomplete cell-type differentiation of the mutant disrupts the balance that controls the initiation of prespore and prestalk differentiation,[29,30] but the molecular details of that pathway are still unknown so it is hard to tell whether they are disrupted in the *rapgapB*$^{-}$ strain.

Previous work identified *rapgapB* as a suppressor of the developmental arrest phenotype of a strain in which the *tgrB1* and *tgrC1* allotypes did not match.[17] None of the suppressor *rapgapB* mutations were found in the genome sequences of wild *D. discoideum* strains. In fact, *rapgapB* is ranked 7,376th in the list of polymorphic genes, indicating that it is highly conserved, unlike *tgrB1* and *tgrC1*, which are ranked 15th and

34th, respectively.[31] There was also no significant correlation between naturally occurring mutations in *rapgapB* and the degree of strain segregation.[4] The high conservation of *rapgapB* probably reflects its essential role in development and might explain that its cheating potential is limited by pleiotropy.[32] Most of the *rapgapB* mutations recovered from that suppressor screen appeared to be loss-of-function alleles, but some alleles were successfully complemented by exogenous expression of a wild-type copy of *rapgapB* whereas others were not, indicating the added complexity of possible recessive versus dominant-negative phenotypic patterns across the allelic spectrum. We therefore used a null allele of *rapgapB* as a reference point for our studies.[20] In parallel, we developed a more scalable CRISPR-Cas9 based knockout strategy to target *rapgapB* in various backgrounds and found that the morphology and prestalk defects of the CRISPR-Cas9 alleles recapitulated that of the insertional knockout. The cheating behavior of the insertional allele was somewhat more aggressive than the CRISPR-Cas9 alleles, in that the cheater produced more spores than the victim and caused more harm to the sporulation efficiency of the wild-type counterpart. Nevertheless, the results obtained with the CRISPR-Cas9 alleles are congruent and therefore validated by the ones obtained with the insertional allele. In both cases, clear costs were exacted upon AX4 because it unilaterally contributed to the common good of the stalk without receiving a reciprocal benefit from *rapgapB*$^{-}$. Moreover, by increasing the sporulation efficiency of *rapgapB*$^{-}$, AX4 increases the population of the cheater mutant in subsequent generations that are definitionally competitors to its own descendants. Therefore, the *rapgapB*$^{-}$ strain is a cheater by the broad definition of a strain that takes advantage of a cooperative social interaction without paying the full cost.[21–23]

Our findings suggest that the cheating behavior conferred by *rapgapB*$^{-}$ is partial. If cheating by *rapgapB*$^{-}$ were stronger, the resulting falsebeard would spread through the population, leading to destabilization or even elimination of the *tgrB1-tgrC1* greenbeard system. The fact that we observe a greenbeard system in *D. discoideum* suggests that falsebeards are not successful in nature. We also note that the *rapgapB* sequence is not polymorphic,[31] suggesting that it is evolving under negative selection. We found that *rapgapB*$^{-}$ exhibits defective morphogenesis and reduced sporulation, and previous studies showed that it has multiple roles, including efficient stalk formation.[20] These observations suggest that *rapgapB* has pleiotropic functions that limit the spread of *rapgapB*$^{-}$ mutations through the population. This finding further supports the hypothesized role of pleiotropy in stabilizing cooperation in *D. discoideum*.[32]

Altogether, the results presented here provide strong empirical support for the falsebeard hypothesis and establish a genetically tractable and quantitative experimental model for further exploration of this phenomenon.

Limitations of the study

The assignment of *rapgapB* to the *tgrB1-tgrC1* genetic pathway is based on the genetic evidence that *rapgapB*-null is a mutual suppressor of *tgrB1* and *tgrC1*. This issue has two potential caveats. First, the phenotypes tested were developmental morphology and spore production. It is possible that other roles of these genes might not be directly related to one pathway. For example, *rapgapB* is a regulator of RapA activity, but that phenotype was not tested. Second, although mutual suppression usually suggests close contact between the gene products, this work has not attempted to characterize protein interactions in the pathway.

This work also concludes that inactivation of *rapgapB* causes cheating. The insertional inactivation of *rapgapB* causes cheating in that the mutant increases its sporulation in the presence of the victim, and the victim sporulation is reduced (Figure S3). The *rapgapB* mutations that were generated by CRISPR caused partial cheating. The mutant was able to increase its sporulation in the presence of the victim, but the victim sporulation was not significantly decreased (Figure 2). The reasons for the difference between the penetrance of these mutations are unknown.

RESOURCE AVAILABILITY

Lead contact

Further information and requests for resources and reagents should be directed to and will be fulfilled by the lead contact, Gad Shaulsky, Department of Molecular and Human Genetics, Baylor College of Medicine, One Baylor Plaza, Houston, TX, 77030, USA (gadi@bcm.edu).

Materials availability

The strains and vectors described here are available upon request from the lead contact.

Data and code availability

- All the data reported in this paper will be shared by the lead contact upon request.
- Any additional information required to reanalyze the data reported in this paper is available from the lead contact upon request.
- This paper does not report original code.

ACKNOWLEDGMENTS

We thank Elizabeth Ostrowski for discussions and for critical evaluation of the manuscript. We thank Susan Hilsenbeck, Director of the Biostatistics and Informatics Shared Resource Core, a Baylor College of Medicine Advanced Technology Core Lab, for expert advice on statistical analysis of the data.

AUTHOR CONTRIBUTIONS

P.L. and G.S. designed the experiments. P.L. performed the experiments. P.K. performed preliminary experiments. P.L. and P.K. generated vectors and strains. M.K.-K. validated key experiments. P.L. and G.S. wrote the manuscript. All the authors reviewed and edited the manuscript.

DECLARATION OF INTERESTS

The authors declare no competing interests.

STAR★METHODS

Detailed methods are provided in the online version of this paper and include the following:

- KEY RESOURCES TABLE
- EXPERIMENTAL MODEL AND STUDY PARTICIPANT DETAILS
  - Strains and strain construction
  - Cell growth and transformation
- METHOD DETAILS
  - Vectors
  - Development, imaging of whole structures, and analysis of mixing experiments
- QUANTIFICATION AND STATISTICAL ANALYSIS
  - Analysis of sporulation in mixing experiments
- ADDITIONAL RESOURCES

SUPPLEMENTAL INFORMATION

Supplemental information can be found online at https://doi.org/10.1016/j.isci.2024.111125.

Received: July 29, 2024
Revised: September 9, 2024
Accepted: October 4, 2024
Published: October 9, 2024

REFERENCES

1. Dawkins, R. (2016). The Selfish Gene, 40th anniversary edition Edition (Oxford University Press).
2. Hamilton, W.D. (1964). The genetical evolution of social behaviour. I. J. Theor. Biol. *7*, 1–16. https://doi.org/10.1016/0022-5193(64)90038-4.
3. Hamilton, W.D. (1964). The genetical evolution of social behaviour. II. J. Theor. Biol. *7*, 17–52. https://doi.org/10.1016/0022-5193(64)90039-6.
4. Gruenheit, N., Parkinson, K., Stewart, B., Howie, J.A., Wolf, J.B., and Thompson, C.R.L. (2017). A polychromatic 'greenbeard' locus determines patterns of cooperation in a social amoeba. Nat. Commun. *8*, 14171. https://doi.org/10.1038/ncomms14171.
5. Katoh-Kurasawa, M., Lehmann, P., and Shaulsky, G. (2024). The greenbeard gene tgrB1 regulates altruism and cheating in Dictyostelium discoideum. Nat. Commun. *15*, 3984. https://doi.org/10.1038/s41467-024-48380-4.
6. Benabentos, R., Hirose, S., Sucgang, R., Curk, T., Katoh, M., Ostrowski, E.A., Strassmann, J.E., Queller, D.C., Zupan, B., Shaulsky, G., and Kuspa, A. (2009). Polymorphic members of the lag gene family mediate kin discrimination in Dictyostelium. Curr. Biol. *19*, 567–572. https://doi.org/10.1016/j.cub.2009.02.037.
7. Hirose, S., Benabentos, R., Ho, H.I., Kuspa, A., and Shaulsky, G. (2011). Self-recognition in social amoebae is mediated by allelic pairs of tiger genes. Science *333*, 467–470. https://doi.org/10.1126/science.1203903.
8. Hirose, S., Chen, G., Kuspa, A., and Shaulsky, G. (2017). The polymorphic proteins TgrB1 and TgrC1 function as a ligand-receptor pair in Dictyostelium allorecognition. J. Cell Sci. *130*, 4002–4012. https://doi.org/10.1242/jcs.208975.
9. Strassmann, J.E., Gilbert, O.M., and Queller, D.C. (2011). Kin discrimination and cooperation in microbes. Annu. Rev. Microbiol. *65*, 349–367. https://doi.org/10.1146/annurev.micro.112408.134109.
10. Gardner, A. (2019). The greenbeard effect. Curr. Biol. *29*, R430–R431. https://doi.org/10.1016/j.cub.2019.03.063.
11. Gardner, A., and West, S.A. (2010). Greenbeards. Evolution *64*, 25–38. https://doi.org/10.1111/j.1558-5646.2009.00842.x.
12. Madgwick, P.G., Belcher, L.J., and Wolf, J.B. (2019). Greenbeard Genes: Theory and Reality. Trends Ecol. Evol. *34*, 1092–1103. https://doi.org/10.1016/j.tree.2019.08.001.
13. Hartman, P.E., and Roth, J.R. (1973). Mechanisms of suppression. Adv. Genet. *17*, 1–105. https://doi.org/10.1016/s0065-2660(08)60170-4.
14. Prelich, G. (1999). Suppression mechanisms: themes from variations. Trends Genet. *15*, 261–266. https://doi.org/10.1016/s0168-9525(99)01749-7.
15. van Leeuwen, J., Pons, C., Boone, C., and Andrews, B.J. (2017). Mechanisms of suppression: The wiring of genetic resilience. Bioessays *39*, 1700042. https://doi.org/10.1002/bies.201700042.
16. Li, C.L.F., Chen, G., Webb, A.N., and Shaulsky, G. (2015). Altered N-glycosylation modulates TgrB1- and TgrC1-mediated development but not allorecognition in Dictyostelium. J. Cell Sci. *128*, 3990–3996. https://doi.org/10.1242/jcs.172882.
17. Li, C.L.F., Santhanam, B., Webb, A.N., Zupan, B., and Shaulsky, G. (2016). Gene discovery by chemical mutagenesis and whole-genome sequencing in Dictyostelium. Genome Res. *26*, 1268–1276. https://doi.org/10.1101/gr.205682.116.
18. Wang, Y., and Shaulsky, G. (2015). TgrC1 Has Distinct Functions in Dictyostelium Development and Allorecognition. PLoS One *10*, e0124270. https://doi.org/10.1371/journal.pone.0124270.
19. Kundert, P., Sarrion-Perdigones, A., Gonzalez, Y., Katoh-Kurasawa, M., Hirose, S., Lehmann, P., Venken, K.J.T., and Shaulsky, G. (2020). A GoldenBraid cloning system for synthetic biology in social amoebae. Nucleic Acids Res. *48*, 4139–4146. https://doi.org/10.1093/nar/gkaa185.
20. Parkinson, K., Bolourani, P., Traynor, D., Aldren, N.L., Kay, R.R., Weeks, G., and Thompson, C.R.L. (2009). Regulation of Rap1 activity is required for differential adhesion, cell-type patterning and morphogenesis in Dictyostelium. J. Cell Sci. *122*, 335–344. https://doi.org/10.1242/jcs.036822.
21. Foster, K.R., Parkinson, K., and Thompson, C.R.L. (2007). What can microbial genetics teach sociobiology? Trends Genet. *23*, 74–80. https://doi.org/10.1016/j.tig.2006.12.003.
22. Ghoul, M., Griffin, A.S., and West, S.A. (2014). Toward an evolutionary definition of cheating. Evolution *68*, 318–331. https://doi.org/10.1111/evo.12266.
23. West, S.A., Griffin, A.S., Gardner, A., and Diggle, S.P. (2006). Social evolution theory for microorganisms. Nat. Rev. Microbiol. *4*, 597–607. https://doi.org/10.1038/nrmicro1461.
24. Ennis, H.L., Dao, D.N., Pukatzki, S.U., and Kessin, R.H. (2000). Dictyostelium amoebae lacking an F-box protein form spores rather than stalk in chimeras with wild type. Proc. Natl. Acad. Sci. USA *97*, 3292–3297. https://doi.org/10.1073/pnas.97.7.3292.
25. Strassmann, J.E., and Queller, D.C. (2011). Evolution of cooperation and control of cheating in a social microbe. Proc. Natl. Acad. Sci. USA *108*, 10855–10862. https://doi.org/10.1073/pnas.1102451108.
26. Strassmann, J.E., Zhu, Y., and Queller, D.C. (2000). Altruism and social cheating in the social amoeba Dictyostelium discoideum. Nature *408*, 965–967. https://doi.org/10.1038/35050087.
27. Rosengarten, R.D., Santhanam, B., Fuller, D., Katoh-Kurasawa, M., Loomis, W.F., Zupan, B.,

and Shaulsky, G. (2015). Leaps and lulls in the developmental transcriptome of Dictyostelium discoideum. BMC Genom. *16*, 294. https://doi.org/10.1186/s12864-015-1491-7.

28. Hilbi, H., and Kortholt, A. (2019). Role of the small GTPase Rap1 in signal transduction, cell dynamics and bacterial infection. Small GTPases *10*, 336–342. https://doi.org/10.1080/21541248.2017.1331721.
29. Loomis, W.F. (1993). Lateral inhibition and pattern formation in Dictyostelium. Curr. Top. Dev. Biol. *28*, 1–46. https://doi.org/10.1016/s0070-2153(08)60208-2.
30. Shaulsky, G., and Loomis, W.F. (1993). Cell type regulation in response to expression of ricin A in Dictyostelium. Dev. Biol. *160*, 85–98. https://doi.org/10.1006/dbio.1993.1288.
31. Ostrowski, E.A., Shen, Y., Tian, X., Sucgang, R., Jiang, H., Qu, J., Katoh-Kurasawa, M., Brock, D.A., Dinh, C., Lara-Garduno, F., et al. (2015). Genomic signatures of cooperation and conflict in the social amoeba. Curr. Biol. *25*, 1661–1665. https://doi.org/10.1016/j.cub.2015.04.059.
32. Foster, K.R., Shaulsky, G., Strassmann, J.E., Queller, D.C., and Thompson, C.R.L. (2004). Pleiotropy as a mechanism to stabilize cooperation. Nature *431*, 693–696. https://doi.org/10.1038/nature02894.
33. Knecht, D.A., Cohen, S.M., Loomis, W.F., and Lodish, H.F. (1986). Developmental regulation of Dictyostelium discoideum actin gene fusions carried on low-copy and high-copy transformation vectors. Mol. Cell Biol. *6*, 3973–3983. https://doi.org/10.1128/mcb.6.11.3973.
34. Sarrion-Perdigones, A., Gonzalez, Y., and Venken, K.J.T. (2022). Synthetic Assembly DNA Cloning of Multiplex Hextuple Luciferase Reporter Plasmids. Methods Mol. Biol. *2524*, 409–432. https://doi.org/10.1007/978-1-0716-2453-1_32.
35. de Winter, J. (2013). Using the Student's t-test with extremely small sample sizes. Practical Assess. Res. Eval. *18*, 10. https://doi.org/10.7275/e4r6-dj05.

STAR★METHODS

KEY RESOURCES TABLE

REAGENT or RESOURCE	SOURCE	IDENTIFIER
Chemicals		
Hygromycin B	Invitrogen	Cat # 10687010
Geneticin (G418)	Gibco	Cat # 10131-035
Blasticidin S	Gibco	Cat #R210-01
Experimental models: organisms/strains		
Dictyostelium discoideum AX4	Dicty Stock Center	http://dictybase.org/StockCenter/StockCenter.html DBS0235552
AX4 *tgrB1*$^{-}$	This study; See Table S2	
AX4 *tgrC1*$^{-}$ (WGdel)	Dicty Stock Center	http://dictybase.org/StockCenter/StockCenter.html DBS0304821
AX4 *rapgapB*$^{-}$	This study; See Table S2	
AX4 *rapgapB*$^{-}$ *tgrB1*$^{-}$ Clone 1	This study; See Table S2	
AX4 *rapgapB*$^{-}$ *tgrB1*$^{-}$ Clone 2	This study; See Table S2	
AX4 *rapgapB*$^{-}$ *tgrC1*$^{-}$ Clone 1	This study; See Table S2	
AX4 *rapgapB*$^{-}$ *tgrC1*$^{-}$ Clone 2	This study; See Table S2	
AX4-R/G	This study; See Table S2	
AX4 *rapgapB*$^{-}$ GFP	This study; See Table S2	
AX4 *rapgapB*$^{-}$ mCherry	This study; See Table S2	
AX4 *rapgapB*$^{-}$ R/G	This study; See Table S2	
AX4 $B1^{AX4}C1^{AX4}$ RFP (DBS0349736)	This study; See Table S2	
AX4 $B1^{QS31}C1^{QS31}$ RFP (DBS0349747)	This study; See Table S2	
AX4 $B1^{QS31}C1^{QS31}$ GFP	Dicty Stock Center	http://dictybase.org/StockCenter/StockCenter.html DBS0349746
AX4 $B1^{QS31}C1^{QS31}$ *rapgap*$^{-}$ RFP	This study; See Table S2	
AX4 $B1^{QS31}C1^{QS31}$ *rapgap*$^{-}$ GFP	This study; See Table S2	
Oligonucleotides		
5′ AATGTTTTCA CATTGTGAAG GATATAG 3′	Sigma Aldrich custom order; See Table S3	rapgapB_amp_F
5′ CTCATTTTAA GGAATGATCT TG 3′	Sigma Aldrich custom order; See Table S3	rapgapB_amp_R
5′ CTCATTTTAA GGAATGATCT TG 3′	Sigma Aldrich custom order; See Table S3	rapgapB Seq
5′ AAGTCTCAAT ATGTGGCTC 3′	Sigma Aldrich custom order; See Table S3	tgrB1_amp_F
5′ ATTGTATTTG ATTTATATTC ACC 3′	Sigma Aldrich custom order; See Table S3	tgrB1_amp_R
5′ CATTCTTAAA GACACCAACC CTAG 3′	Sigma Aldrich custom order; See Table S3	tgrB1 Seq
Recombinant DNA		
pDGB_α2[CRISPR1_tgrB1]	Our laboratory	Katoh-Kurasawa et al.[5]
pDGB_α2[CRISPR1_rapgapBsg2]	Our laboratory	Kundert et al.[19]
pUPD2	Our laboratory	Kundert et al.[19]

(*Continued on next page*)

Continued

REAGENT or RESOURCE	SOURCE	IDENTIFIER
pDGB_A2N	Our laboratory	Kundert et al.[19]
pDGB_A2N_sgRNA-TinselPurple:act8t	Our laboratory	This study
pDGB_A1_act15p_SpCas9-SV40NLS-eGFP_act8t	Our laboratory	Kundert et al.[19]
pDGB_Ω2H	Our laboratory	Kundert et al.[19]
pDGB_Ω2H_CRISPR1	Our laboratory	This study

EXPERIMENTAL MODEL AND STUDY PARTICIPANT DETAILS

Strains and strain construction

All the *D. discoideum* strains were generated by transformation of AX4[33] or its derivatives as detailed in the key resources table and in Table S2.

Cell growth and transformation

We maintained *D. discoideum* cells at 22°C in HL5 nutrient broth in submerged culture and grew them for transformation and development in shaking suspension at 200 RPM with the adequate antibiotics (10 μg/ml G418, 5 μg/ml Blasticidin S, or 100 μg/ml Hygromycin B) as indicated in the key resources table and Table S2, and as previously described.[6] We transformed the cells by electroporation, cloned by plating in association with bacteria and identified the desired clones by PCR analysis. Before each experiment, we grew the cells at the logarithmic phase without antibiotics for 24 h. Mutagenesis by CRISPR/Cas9 was performed as described.[19] Briefly, we used CRISPOR to design sgRNA's (http://crispor.tefor.net/). We ordered custom-made single-stranded oligonucleotides as detailed in the key resources table and in Table S3, annealed them and cloned them into the GoldenBraid vector system. We then transformed *D. discoideum* cells and selected for the desired clones after 5–7 days of transient selection. We validated all the transformed strains by PCR and sequencing of the relevant genes or segments. The relevant sequences are provided in Data S1. The PCR primers used for each diagnostic amplification and sequencing oligonucleotides for CRISPR validation are listed in the key resources table and in Table S3.

METHOD DETAILS

Vectors

We used the previously published vector pDGB_α2[CRISPR1_tgrB1][5] to mutate the *tgrB1* gene in the AX4 strain. We used the previously published vector pDGB_α2[CRISPR1_rapgapBsg2][19] to mutate the *rapgapB* gene in the neomycin-sensitive strains AX4, *tgrB1*$^{-}$ *and tgrC1*$^{-}$. To mutate the *rapgapB* gene in strains that were already neomycin-resistant (AX4-GFP, AX4-RFP, AX4-R/G, AX4 $B1^{QS31}C1^{QS31}$ GFP, and AX4 $B1^{QS31}C1^{QS31}$ RFP), we constructed a vector containing a hygromycin resistance marker, as follows: We ordered a synthetic DNA segment of 1217bp (gBlock Gene Fragment, Integrated DNA Technologies, Inc. USA) containing 1) the sgRNA expression machinery previously described[19] at base positions 20–183 and 871–1198, 2) the coding sequence of TinselPurple (base positions 184–870), a chromoprotein used for purple-white screening of bacterial transformants as an alternative to blue-white screening using *lacZ*,[34] and 3) GoldenBraid grammar at base positions 1–19 and 1199–1217 to allow domestication into the pUPD2 backbone as described.[19] We then assembled the sgRNA-TinselPurple cassette with the *actin8* terminator as a transcriptional unit into the pDGB_A2N backbone using GoldenBraid. We then assembled the resulting vector pDGB_A2N_sgRNA-TinselPurple:act8t along with the vector pDGB_A1_act15p_SpCas9-SV40NLS-eGFP_act8t into the pDGB_Ω2H backbone, generating pDGB_Ω2H_CRISPR1. We then used the previously published sgRNA targeting exon 1 of *rapgapB* and cloned into the pDGB_Ω2H_CRISPR1 vector as described.[19]

Development, imaging of whole structures, and analysis of mixing experiments

We induced development by washing the cells twice in KK2 buffer (20 mM potassium phosphate, pH6.4) followed by starvation in a humid chamber at 22°C. In mixing experiments, we grew the strains separately, washed the cells separately, counted them, and mixed in equal proportions before depositing them on solid substrates for development. To image developmental structures, we plated cells at a density of 2-5x10^5 cells/cm^2 on 1.5% Noble agar made in KK2. Fluorescence and Differential Interference Contrast (DIC) microscopy images were captured with a Nikon (Tokyo, Japan) Eclipse Ti microscope as described.[19] To measure sporulation and cheating, we plated 1.25x10^6 cells/cm^2 cells on each quarter of a black nitrocellulose filter and placed three replicate quarter filters on one filter pad per sample. We developed the cells for 40 h in a humid chamber, harvested spores into KK2 supplemented with 0.1% NP40 (to eliminate un-sporulated cells) and washed the spores twice with KK2. We counted the spores and captured fluorescence and DIC micrographs of several fields to calculate the sporulation efficiency of each strain in the mix.

QUANTIFICATION AND STATISTICAL ANALYSIS

Analysis of sporulation in mixing experiments

The average of the three-quarter filter counts was reported as one data point. Each experiment was repeated three independent times as reported in Figures 2, 4, and S2. To compare between development in pure population and development in 1:1 mixes, we multiplied the pure population spore counts by 0.5 to scale them with the mixed populations. We then performed one-sided paired T-tests using Microsoft Excel 16.84 to compare pairs of pure and mixed populations. Using a T-test is appropriate in this case considering the number of replications[35] and because the data conform with the assumptions of approximate normality and approximate equality of variance.

ADDITIONAL RESOURCES

This study has not generated additional resources.